Research Article

Precision medicine for patients with salivary gland neoplasms: Determining the feasibility of implementing a next-generation sequencing-based RNA assay in a hospital laboratory

Gloria Hopkins Sura, MD[1,2], Jim Hsu, MD PhD[1], Dina R. Mody, MD[1], Jessica S. Thomas, MD PhD MPH[1]

[1]Department of Pathology and Genomic Medicine, Houston Methodist, Houston, Texas, USA. [2]Department of Anatomic Pathology, Division of Pathology and Laboratory Medicine, The University of Texas MD Anderson Cancer Center, Houston, Texas, USA.

*Corresponding author:

Gloria Hopkins Sura,
Department of Anatomic Pathology, Division of Pathology and Laboratory Medicine, The University of Texas MD Anderson Cancer Center, Houston, Texas, USA.

Email: ghsura@mdanderson.org

ABSTRACT

Objective: Diagnosing neoplasms of the salivary gland is challenging, as morphologic features of these tumors are complex, and well-defined diagnostic categories have overlapping features. Many salivary gland neoplasms are associated with recurrent genetic alterations. The utilization of RNA-based targeted next-generation sequencing (NGS) panels for the detection of cancer-driving translocations and mutations is emerging in the clinical laboratory. Our objective was to conduct a proof-of-concept study to show that in-house molecular testing of salivary gland tumors can enhance patient care by supporting morphologic diagnoses, thereby improving therapeutic strategies such as surgical options and targeted therapies.

Material and Methods: Residual formalin-fixed paraffin-embedded salivary gland neoplasm specimens from a cohort of 17 patients were analyzed with the Archer FusionPlex Pan Solid Tumor v2 panel by NGS on an Illumina NextSeq550 platform.

Results: We identified structural gene rearrangements and single nucleotide variants in our patient samples that have both diagnostic and treatment-related significance. These alterations included *PLAG1, MAML,* and *MYB* fusions and *BRAF*, *CTNNB1*, *NRAS,* and *PIK3CA* mutations.

Conclusion: Our RNA-based NGS assay successfully detected known gene translocations and mutations associated with salivary gland neoplasms. The genetic alterations detected in these tumors demonstrated potential diagnostic, prognostic, and therapeutic value. We suggest that incorporating in-house ancillary molecular testing could greatly enhance the accuracy of salivary gland fine needle aspiration cytology and small biopsies, thereby better guiding surgical decisions and the use of targeted therapies.

Keywords: salivary gland, RNA sequencing, fine-needle aspiration, next-generation sequencing, precision medicine

INTRODUCTION

Neoplasms of the salivary gland are rare, often occur in older adults, and approximately 75% are benign. Fine-needle aspiration cytology (FNAC) is widely accepted as a primary diagnostic test for salivary gland lesions, supported by the Milan System for Reporting Salivary Gland Cytopathology, which provides a standard approach for reporting results and associated risk of

malignancy.[1] Guidelines for the interpretation of surgical resection specimens, such as the World Health Organization Classification of Head and Neck Tumors, recognize over 30 epithelial salivary gland tumors.[2] Despite these frameworks, challenges persist in recognizing and grading salivary gland neoplasms due to their complex morphology and to low- and high-grade neoplasm features overlapping, which complicates risk stratification and can lead to suboptimal patient management.

Genetic alterations in salivary gland neoplasms, such as *MAML2* fusions in mucoepidermoid carcinoma, *MYB* fusions in adenoid cystic carcinoma, *PRKD1* alterations in polymorphous adenocarcinoma, and *ETV6* fusions in secretory carcinoma, can assist in diagnosing challenging cases and selecting targeted therapy. Emerging targetable alterations include *ETV6:NTRK3*, *EML4:ALK*, and *NCOA4:RET* gene fusions, as well as mutations in *PIK3CA*, *NOTCH1*, and *HRAS* and amplifications in *ERBB2*.[3] Utilizing RNA-based, targeted next-generation sequencing (NGS) panels for the detection of cancer-associated translocations and mutations and for expression profiling is increasingly common. Molecular testing of FNAC specimens, small biopsies, and surgical resection samples can enhance diagnosis, predict the risk of malignancy more accurately, guide surgical treatment decisions (e.g., whether to perform conservative surgery, a neck lymph node dissection, or facial nerve sacrifice), and select for targeted therapy.

In this study, total nucleic acid was extracted from stored formalin-fixed paraffin-embedded (FFPE) tissue blocks and evaluated using the Archer FusionPlex Pan Solid Tumor v2 panel (Integrated DNA Technologies, Boulder, Colorado, USA) by NGS on an Illumina NextSeq550 platform (Illumina, San Diego, California, USA) in our molecular diagnostics laboratory at Houston Methodist, Texas Medical Center, Houston, Texas. This panel targets 137 genes associated with translocations in solid organ tumors, including salivary gland neoplasms. It detects structural gene rearrangement (without prior knowledge of the breakpoint site or translocation partner), deletions, insertions, single nucleotide variants, and gene expression levels. This panel is an expanded version of the current validated panel used for the detection of gene rearrangements in lung, thyroid, and other solid organ tumors in our laboratory, allowing for specimens from the different assay types to be batched on the same run, offering a cost-effective solution for rare specimens. The study aimed to assess the feasibility of using a large RNA-based sequencing panel in a clinical laboratory setting to potentially enable in-house testing for salivary gland neoplasms and improve turnaround time and access to personalized treatments. We developed this proof of concept in hopes of implementing molecular testing on FNAC specimens and small biopsies at initial diagnosis.

MATERIAL AND METHODS

Ethical approval and informed consent

Human subject research was involved in this study and was carried out in compliance with the Helsinki Declaration with review and oversight from the Institutional Review Board of the Houston Methodist Research Institute.[4] The study was approved for a waiver of informed consent in November 2022 by the Institutional Review Board at Houston Methodisdt Research Institute (protocol 00035700).

Sample cohort

We selected 17 salivary gland neoplasm cases received by the Department of Pathology and Genomic Medicine at Houston Methodist for routine diagnostic evaluation that had adequate remaining material for molecular testing. Cases were identified using case-insensitive free-text keyword searches of system-wide anatomic pathology interpretations for phrases corresponding to known salivary gland neoplasm (e.g., "acinic cell carcinoma," "mucoepidermoid carcinoma," and "pleomorphic adenoma") and manually reviewed to remove cases that were negative for malignancy (e.g., Warthin's tumor and sialadenitis) as well as malignancies of non-salivary gland origin (e.g., metastatic head-and-neck squamous cell carcinoma). None of the specimens had previously received molecular testing. The date range used for the search spanned January 1, 2020, to December 31, 2022. The specimens, all from FFPE tissue blocks, ranged from 1 to 3 years old at the time of nucleic acid extraction.

Total nucleic acid isolation

Residual FFPE tissue blocks were freshly cut as 10-micrometer-thick sections and mounted on uncharged glass slides. A pathologist (GHS) marked hematoxylin and eosin-stained slides for tumor location and estimated tumor-to-normal ratios. Manual macro-dissection was performed to ensure a tumor burden of at least 20%. Unstained slides were scraped for total nucleic acid extraction using the Agencourt FormaPure FFPE tissue kit (Beckman Coulter, Brea, California, USA). Quantification and estimation of purity of nucleic acids were performed using the Qubit fluorometric assay (ThermoFisher Scientific, Waltham, Massachusetts, USA).

Library preparation and NGS

Library preparation for the Archer FusionPlex Pan Solid Tumor v2 was performed according to the manufacturer's protocol using 150 ng of input RNA. SeraCare Tumor Fusion RNA RM v4 and SeraCare *NTRK* Tumor Fusion (LGC Clinical Diagnostics, Milford, Massachusetts, USA) reference materials containing known transcript levels of clinically

relevant RNA fusions were used as positive controls in each run. Molecular-grade water was used as a negative control. If the controls were invalid, then the entire run would be deemed invalid. Library quantification was performed using the Kapa Biosystems quantitative polymerase chain reaction (PCR) kit for Illumina (Kapa Biosystems, Wilmington, Massachusetts, USA).

Sequencing was performed on an Illumina NextSeq550 Sequencing System using a NextSeq Mid Output 300 v2.5 cycle cartridge (Illumina, San Diego, California, USA). Libraries were sequenced in paired-end configuration using a read length of 2 × 151 base pairs, resulting in up to 260 million reads passing filter, with an output of 30–39 Gb per flow cell. The NextSeq550 System Mid-Output Kit is estimated to allow for up to 96 amplicon panels, 12 enrichment panels, or 3 exomes. The expected sequencing quality score for a read length of 2 × 150 base pairs was >75% bases per run higher than Q30, correlating to a probability of incorrect base calling at 1 in 1000 or an inferred base call accuracy of 99.9%.

Target genes tested for fusion, splicing, exon-skipping, and SNV/indel

YWHAE, YAP1, WWTR1, VGLL2, USP6, TMPRSS2, THADA, TFE3, TFEB, TFG, TERT, TCF12, STAT6, SS18L1, SS18, RSPO3, RSPO2, ROS1, RET, RELA, RAD51B, PRKD3, PRKD2, PRKD1, PRKCB, PRKCA, PRKACB, PRKACA, PRDM10, PPARG, PLAG1, PKN1, PIK3CA, PHKB, PHF1, PDGFRB, PDGFRA, PDGFD, PDGFB, PAX8, PAX3, NUMBL, NUTM1, NTRK3, NTRK2, NTRK1, NRG1, NRAS, NR4A3, NOTCH2, NOTCH1, NFIB, NFE2L2, NFATC2, NCOA3, NCOA2, NCOA1, MYOD1, MYC, MYBL1, MYB, MUSK, MSMB, MN1, MKL2, MGEA5, MET, MEAF6, MDM2, MBTD1, MAST2, MAST1, MAP2K1, MAML2, KRAS, JAZF1, JAK3, JAK2, INSR, IGF1R, IDH2, IDH1, HRAS, HMGA2, GRB7, GLI1, FUS, FOXR2, FOXO4, FOXO1, FOSB, FOS, FGR, FGFR3, FGFR2, FGFR1, FGF1, EWSR1, ETV6, ETV5, ETV4, ETV1, ESRRA, ESR1, ERG, ERBB4, ERBB2, EGFR, EGF, EPC1, DNAJB1, CTNNB1, CSF1R, CSF1, CRTC1, CIC, CD274, CCND1, CCNB3, CAMTA1, BRD4, BRD3, BRAF, BCOR, AXL, ARHGAP6, ARHGAP26, AR, ALK, AKT3, AKT2, AKT1, ACVR2A, KIT.

Sequencing data analysis

The binary base call (BCL) sequencing output files were processed using a customized bioinformatic pipeline developed in-house, the Houston Methdodist Variant Viewer, and analyzed by the proprietary Archer Analysis software, version 6.2.7 (Integrated DNA Technologies, Boulder, Colorado, USA).[5] Components of our in-house bioinformatic pipeline using the Agilent Genomics Toolkit

(AGeNT) were designed to generate deduplicated FASTQ files compatible with Archer Analysis. Briefly, BCL Convert v4.0.3 (Illumina, San Diego, California, USA) was used for demultiplexing and generation of FASTQ format files [Table 1]. Unique molecular identifier incorporation was performed with default parameters (stringency criteria of 0.9). Adapter trimming (AdapterRead1 and AdapterRead2) was disabled. FASTQ files were exported to a uniquely identifiable folder name with sample ID [Table 1].

The AGeNT consists of multiple modules: AGeNT Trimmer, to trim remaining adapter sequences that were skipped by BCL Convert, and AGeNT CReaK, to create consensus, deduplicated read pairs from aligned reads. CreaK was run using the parameters "consensus_mode="HYBRID"" and "remove-dup-mode" as recommended per Agilent documentation [Table 1]. During assay design, Picard was used with the "bait=target=covered" parameter to generate

Table 1: Relevant parameters for the bioinformatic pipeline used for the analysis of the Archer FusionPlex Pan Solid Tumor v2 assay.

Module	Parameters
BCL Convert	Specified in Cron Script (relevant parameters include disabling AdapterRead1 and AdapterRead2 trimming)
Trimmer	java-jar trimmer-3.0.5.jar \ - fq1 ${fastq1} \ - fq2 ${fastq2} \ - v2 \ - out $/trimmed_fastq/${sample}_trimmed
BWA MEM	"/bwa mem \ - t ${mem_threads} \ - C \ ${ref_genome} \ ${fastq1_trimmed} \ ${fastq2_trimmed} \ - R ""@RG\tID:${sample}\tSM:${sample}\tPL: ILLUMINA\tLB: XT"" | \ /storage/apps/opt/samtools_1_15/bin/ samtools view \ --threads ${view_threads} \ - bf ${view_flag} \ > $/bam/${sample}.bam"
CReaK	java -Xm×40G -jar/storage/apps/opt/ AGeNT_3.0.6/agent/lib/creak-1.0.5.jar \ - b ${CGP_bed} \ - c ${consensus_mode} \ - o ${bam_deduplicated} \ - f \ - F \ - r \ ${bam}

BCL: Binary base call, BWA MEM: Burrows-Wheeler Aligner-maximum exact matches, CReaK: Consensus Read Kit

run-to-run quality control metrics, and alignment was performed with BWA MEM v0.7.12 using GCRh38_no_alt as the reference genome [Table 1].

Archer Analysis software was used to process the deduplicated FASTQ files and generate the output list of SNV/indels and fusions. "Illumina (paired)" was selected as the platform. "RNA Fusion" and "RNA SNP/InDel" were selected as analysis types, and "FusionPlex Pan Solid Tumor v2 18091 v1.1" was used for the panel. All other proprietary parameters were usedas default.

To pass the quality control statistics, the total number of paired-end sequencing reads was required to be at least 1.5 million. The sequencing data for each fusion and variant call were manually reviewed for accuracy. We reported only "strong-evidence" fusion and variant calls. "Strong-evidence" fusion calls, as defined by the Archer software, are as follows: a minimum of 5 reads spanning the fusion breakpoint must be present; the proportion of reads spanning the breakpoint that supports the candidate fusion relative to the total number of reads spanning the fusion region must be at least 10%; a minimum of 3 unique primer start sites within the population of reads spanning the breakpoint supporting the called fusion must be present; and the candidate fusion must be present in the database of previously reported fusions, namely the Quiver Fusion Database (Integrated DNA Technologies, Boulder, Colorado, USA) or meet all other "strong-evidence" criteria. In addition, we excluded exon-intron fusions, paralogs (per Ensemble database), mispriming, and low-confidence alignments (per BLAST: Basic Local Alignment Search Tool).[6,7] Fusion calls that were detected but did not meet all of the above criteria were considered "weak-evidence" fusions and not reported. Mutation calls were considered reportable when there was a minimum of 5 reads covering the mutant allele, 10 unique start sites, and at least 10% mutant allele frequency. Moreover, for a fusion or a variant to be considered reportable in this study, the corresponding control samples were required to pass equivalent quality control metrics.

RESULTS

Genetic alterations with diagnostic and therapeutic implications, including strong-evidence translocations and variants, were detected in 8 of the 17 specimens [Table 2]. The molecular testing results were concordant with the patient's clinical presentation and pathologic diagnosis. These alterations included *PLAG1, MAML,* and *MYB* fusions and *BRAF*, *CTNNB1*, *NRAS,* and *PIK3CA* mutations. In addition, cases were batched and sequenced simultaneously with samples prepared in our in-house validated FusionPlex comprehensive thyroid and lung (CTL) assay kit, which detects rearrangements in 13 genes including *ALK*, *RET*, *ROS1*, *BRAF*, *FGFR1/2/3*, *NTRK1/2/3*, and *MET*, and passed all QC metrics.

Individual case review

Adenoid cystic carcinoma with high-grade transformation: MYB::NFIB t(6;9) & PIK3CA p.H1047R

This 2.5 cm tumor in the left submandibular gland of a 65-year-old man, identified as adenoid cystic carcinoma with high-grade transformation and dedifferentiation, exhibited cribriform and solid growth patterns [Figure 1a-c]. Histology showed necrosis, apoptotic bodies, and atypical mitotic figures with foci of high-grade transformation. The tumor infiltrated surrounding adipose tissue and skeletal muscle, with peri- and intraneural invasion but no lymphovascular invasion. Extensive neck dissection revealed no lymph node metastasis. Immunohistochemical stains were strongly positive for vimentin, cytokeratin 7, cytokeratin 5/6, CD117, and SOX10 while weakly positive for S100. Smooth muscle actin was strongly expressed in a subset of tumor cells but was negative in the areas of high-grade infiltrative carcinoma. The high-grade component showed moderate p53 overexpression and a Ki-67 index >50%. Molecular testing identified a *MYB::NFIB* fusion and a *PIK3CA* p.H1047R mutation [Figure 1d].

Adenoid cystic carcinoma is a biphasic neoplasm with various growth patterns, including cribriform, tubular, and solid types.[1] *MYB* fusions, including *MYB::NFIB*, are common, occurring in over 60% of cases.[8] Although *MYB* immunohistochemistry has low specificity and sensitivity, it can assist in diagnosis when combined with molecular testing. *MYB* and *MYBL1* gene alteration detection can aid in the diagnosis of adenoid cystic carcinomas, especially when poorly differentiated morphology can make it difficult to diagnose based on morphology and immunohistochemistry alone. *PIK3CA* alterations have prognostic and therapeutic implications, with inhibitors currently under development.[9]

Myoepithelial carcinoma ex pleomorphic adenoma: LIFR::PLAG1 t(5;8)

This 3.5 cm tumor of the left parotid in a 70-year-old woman was initially diagnosed as a neoplasm of uncertain malignant potential on FNAC. The final diagnosis, after surgical resection, was myoepithelial carcinoma ex pleomorphic adenoma [Figure 2a and b]. The tumor displayed multinodular growth, marked cytologic atypia, and an immunohistochemical profile positive for S100, SOX10, vimentin, and p53 while negative for cytokeratin 7 and EMA. No lymphovascular invasion or metastatic disease in lymph nodes was identified. Molecular testing revealed an *LIFR::PLAG1* fusion [Figure 2c].

Myoepithelial carcinomas, the second most common type of carcinoma arising within a pleomorphic adenoma, can be clinically aggressive. *PLAG1* rearrangements, including

Table 2: List of salivary gland tumor cases with corresponding RNA sequencing results.

| Sample #	Histologic Diagnosis	RNA Sequencing Results	Tumor Location
1	Adenoid cystic carcinoma ex pleomorphic adenoma	*HRAS* c. 181C >A; p.Gln61Lys	Parotid gland
2	Acinic cell carcinoma	No reportable alterations	Parotid gland
3	Low-grade salivary gland-type adenocarcinoma of the lung	No reportable alterations	Lung
4	Mucoepidermoid carcinoma, low-to-intermediate grade	No reportable alterations	Tongue base
5	Adenoid cystic carcinoma	No reportable alterations	Parotid gland
6	Myoepithelial carcinoma ex pleomorphic adenoma	*LIFR::PLAG1*	Parotid gland
7	Salivary duct carcinoma	No reportable alterations	Parotid gland
8	Pleomorphic adenoma and carcinoma	*CTNNB1::PLAG1*	Parotid gland
9	Salivary duct carcinoma	BRAF c. 1799T >A; p.Val600Glu	Parotid gland
10	Pleomorphic adenoma	No reportable alterations	Parotid gland
11	Adenoid cystic carcinoma with high-grade transformation	*MYB::NFIB* *PIK3CA* c. 3140A >G; p.His1047Arg	Submandibular gland
12	Mucoepidermoid carcinoma, low grade	No reportable alterations	Buccal mucosa
13	Basal cell adenoma	*CTNNB1* c. 104T >C; p.Ile35Thr	Parotid gland
14	Mucoepidermoid carcinoma, low grade	*CRTC1::MAML2*	Hard palate
15	Mucoepidermoid carcinoma, high grade	No reportable alterations	Parotid gland
16	Mucoepidermoid carcinoma, intermediate grade	*CRTC1::MAML2*	Hard palate
17	Myoepithelial-rich/cellular pleomorphic adenoma	No reportable alterations	Parotid gland
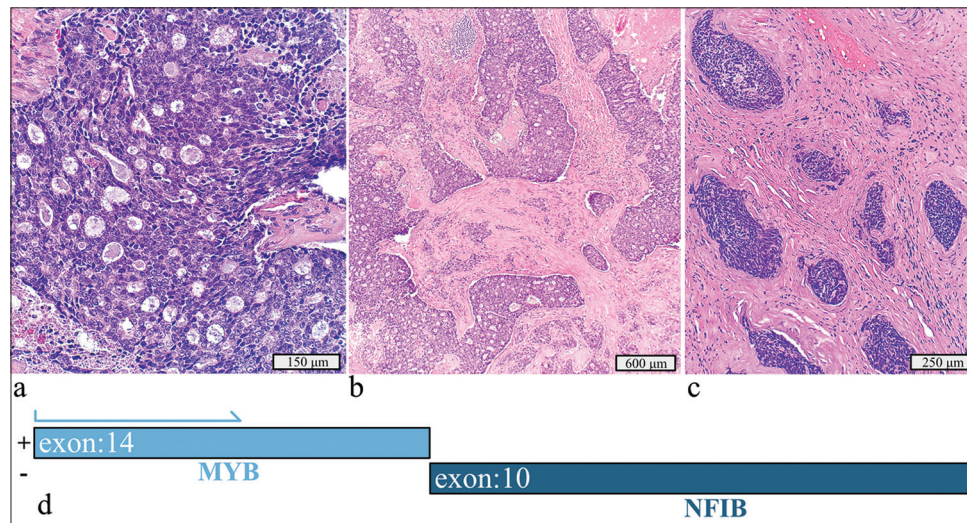
Figure 1: Adenoid cystic carcinoma with high-grade transformation with a detected *MYB::NFIB* fusion and *PIK3CA* p.H1047R mutation. (a) Hematoxylin and eosin stain, 20× objective. (b) Hematoxylin and eosin stain, 4× objective. (c) Hematoxylin and eosin stain demonstrating the dedifferentiation component invading soft tissue, 10× objective. (d) Schematic view of the detected *MYB::NFIB* fusion demonstrating anchored primer regions spanning exon 10 of *NFIB* and exon 14 of *MYB*. The "+" denotes the gene-specific anchored primer (first strand) and (-) the universal primer (second strand). The arrow represents the gene-specific primer.

CTNNB1, LIFR, and *FGFR1* fusion partners, can help confirm the diagnosis of pleomorphic adenoma but cannot distinguish additional carcinoma components. Studies have shown that morphologic mimics of pleomorphic adenoma
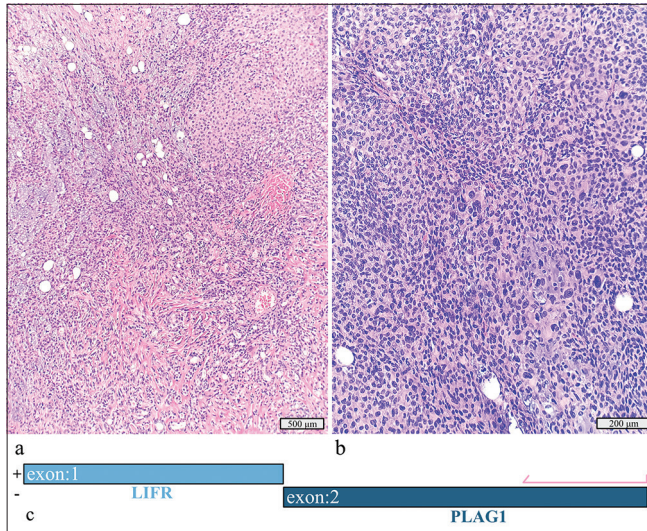
Figure 2: Myoepithelial carcinoma ex pleomorphic adenoma with a detected *LIFR::PLAG1* fusion. (a) Hematoxylin and eosin stain, ×10 objective. (b) Hematoxylin and eosin stain, ×20 objective. (c) Schematic view of the detected *LIFR::PLAG1* fusion demonstrating anchored primer regions spanning exon 2 of *PLAG1* and exon 1 of *LIFR*. The "+" denotes the gene-specific anchored primer (first strand) and () the universal primer (second strand). The arrow represents the gene-specific primer.

and *de novo* carcinomas are negative for the common fusions *PLAG1* and *HMGA2*.[10]

Mucoepidermoid carcinoma, well-differentiated, ex pleomorphic adenoma: CTNNB1::PLAG1 t(3;8)

In a 52-year-old man, a 4.8 cm tumor located in the left parotid gland was initially diagnosed as a pleomorphic adenoma on FNAC. Surgical resection revealed well-differentiated mucoepidermoid carcinoma arising from a pleomorphic adenoma [Figure 3a]. No lymphovascular or perineural invasion or lymph node metastasis was identified. Molecular testing revealed a *CTNNB1::PLAG1* rearrangement [Figure 3b].

The *CTNNB1::PLAG1* fusion indicated origin from a pleomorphic adenoma but did not aid in further classification.

Salivary duct carcinoma: BRAF p.V600E

A 3.0 cm tumor in the left superficial parotid gland of a 73-year-old man was identified as a salivary duct carcinoma after total parotidectomy [Figure 4a and b]. The tumor exhibited high-grade features, infiltrated surrounding tissues, and showed extensive lymphovascular and perineural invasion with metastasis in 3 of 11 lymph nodes. Immunohistochemistry revealed strong positivity for androgen receptor and GATA3 and negative human epidermal growth factor receptor 2 amplification by
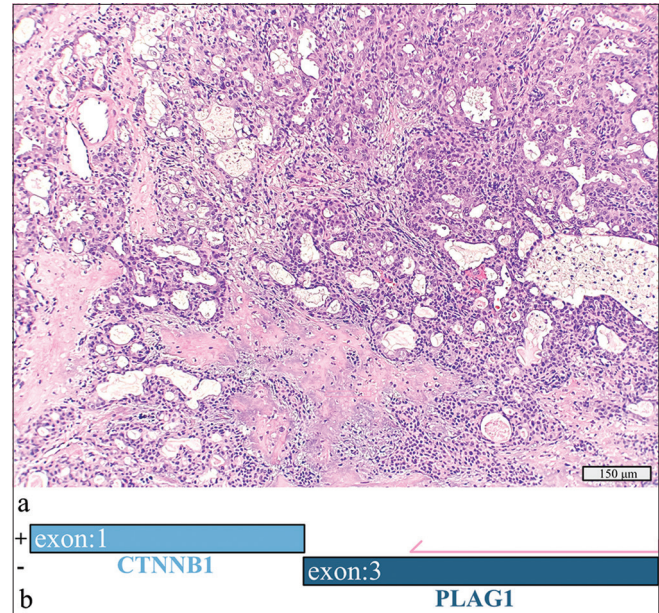
Figure 3: Mucoepidermoid carcinoma, well-differentiated ex-pleomorphic adenoma with a detected *CTNNB1::PLAG1* fusion. (a) Hematoxylin and eosin stain, 20× objective. (b) Schematic view of the *CTNNB1::PLAG1* fusion demonstrating anchored primer regions spanning exon 3 of *PLAG1* and exon 1 of *CTNNB1*. The "+" denotes the gene-specific anchored primer (first strand) and (-) the universal primer (second strand). The arrow represents the gene-specific primer.
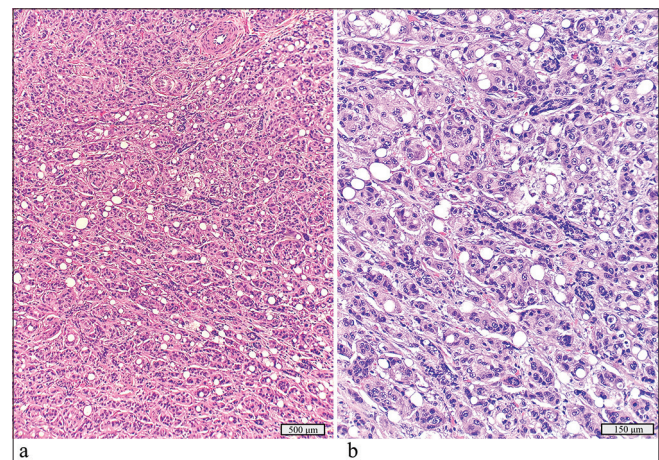
Figure 4: Salivary duct carcinoma with a detected *BRAF* p.V600E mutation. (a) Hematoxylin and eosin stain, ×10 objective. (b) Hematoxylin and eosin stain, ×40 objective.

fluorescent *in situ* hybridization (FISH). RNA sequencing detected a *BRAF* p.V600E mutation.

Comprehensive molecular profiling of salivary duct carcinomas has revealed *BRAF* p.V600E alterations in 3–13% of these neoplasms.[11] Targeted *BRAF* therapy is currently under investigation and has shown promising results in salivary gland carcinoma patients, including initial response to therapy and stable disease.[12]

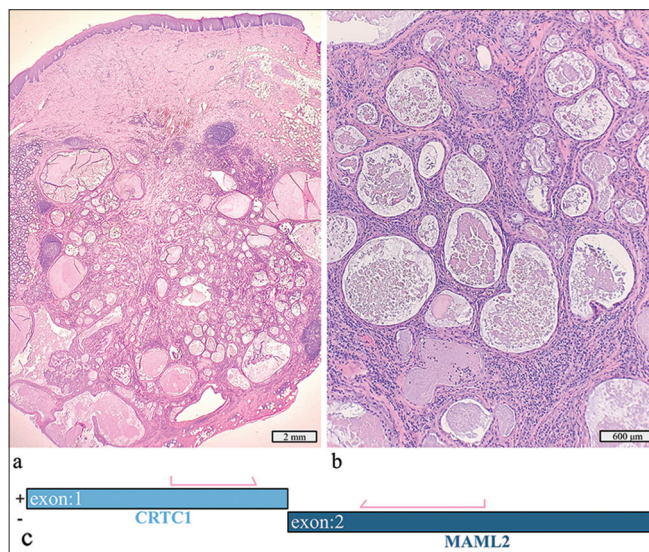### Mucoepidermoid carcinoma, low grade: CRTC1::MAML2 t(11;19)

A 1.6 cm left palatal mass in a 33-year-old man was initially diagnosed as a low-grade cystic neoplasm on FNAC. Surgical excision revealed a well-circumscribed mucoepidermoid carcinoma with cystic areas [Figure 5a and b]. No anaplasia, necrosis, or mitotic activity was seen. Molecular testing detected a *CRTC1::MAML2* fusion [Figure 5c].

The *CRTC1::MAML2* fusion is the most frequent genetic aberration in mucoepidermoid carcinoma, particularly of low-to-intermediate grade and can aid in distinguishing these tumors from well-differentiated tumors from benign salivary gland cysts. *MAML2* fusions are more often detected in low-to-intermediate grade neoplasms.[13,14]

Mucoepidermoid carcinoma, intermediate grade: CRTC1::MAML2 t(11;19) fusion

A 3.5 cm left palatal lesion in a 39-year-old man, present for approximately 5 years, was diagnosed with a squamous papilloma on initial core biopsy. Excision revealed an intermediate-grade mucoepidermoid carcinoma with cystic spaces and mixed cell types [Figure 6a]. No lymphovascular or perineural invasion was found. RNA sequencing revealed a *CRTC1::MAML2* fusion [Figure 6b].

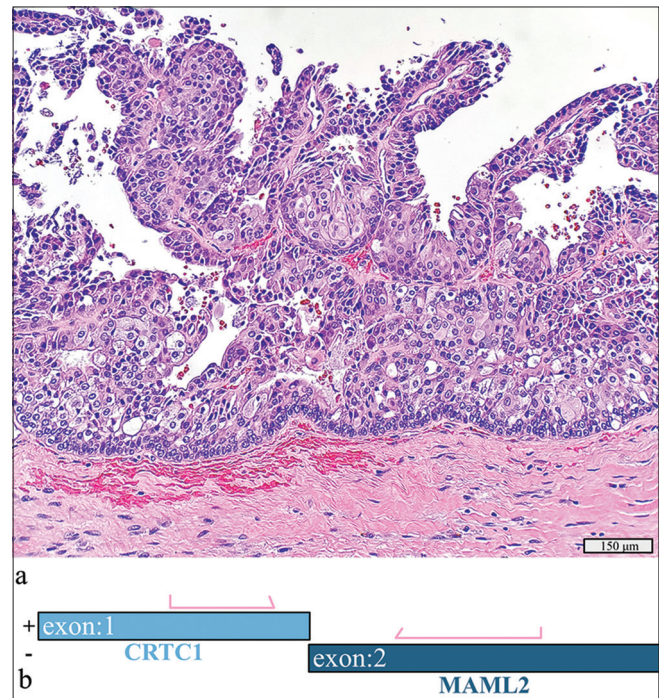The detection of *MAML* fusions can help diagnose cases that are morphologically challenging, such as in this case where the initial biopsies were predominantly squamous in appearance. Though promising, no targeted treatments for *MAML2*-altered neoplasms are currently available.[13,14]

Adenoid cystic carcinoma ex pleomorphic adenoma: HRAS p.Q61L

A 2.7 cm cystic mass in the right parotid gland of a 70-year-old initially showed only cyst contents on FNAC. After parotidectomy, the diagnosis was adenoid cystic carcinoma ex pleomorphic adenoma, with the carcinoma component measuring 1.9 cm [Figure 7a and b]. The tumor showed tubular patterns and was positive for CD117 and p63, with no extra parotid extension or lymph node metastasis. Molecular testing detected an *HRAS* p.Q61L mutation.

HRAS mutations have potential as a predictive biomarker for immunotherapy, though no approved therapies for salivary gland neoplasms exist to date. Ongoing studies including farnesyl transferase inhibitors (e.g., tipifarnib) have shown some promise; for example, one phase II study demonstrated disease stabilization in half of patients with recurrent or metastatic *HRAS*-mutated salivary gland carcinomas.[15,16]


Figure 5: Low-grade mucoepidermoid carcinoma with a detected *CRTC1::MAML2* fusion. (a) Hematoxylin and eosin stain, ×4 objective. (b) Hematoxylin and eosin stain, ×10 objective. (c) Schematic view of the detected *CRTC1::MAML2* fusion demonstrating anchored primer regions spanning exon 1 of *CRTC1* and exon 2 of *MAML1*. The "+" denotes the gene-specific anchored primer (first strand) and (−) the universal primer (second strand). The arrows represent the gene-specific primer.

Figure 6: Intermediate-grade mucoepidermoid carcinoma with a detected *CRTC1::MAML2* fusion. (a) Hematoxylin and eosin stain, ×20 objective. (b) Schematic view of the detected *CRTC1::MAML2* fusion demonstrating anchored primer regions spanning exon 1 of *CRTC1* and exon 2 of *MAML2*. The "+" denotes the gene-specific anchored primer (first strand) and (−) the universal primer (second strand). The arrows represent the gene-specific primer.
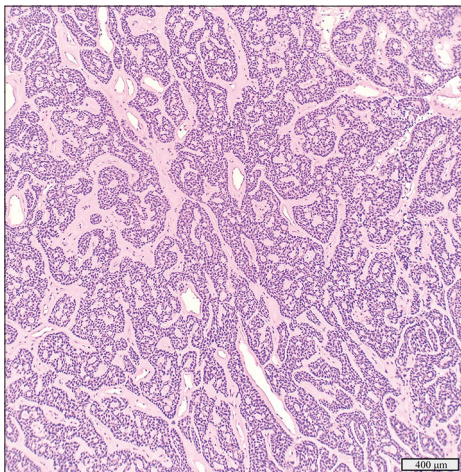
Basal cell adenoma: CTNNB1 p.I35T

A 1 cm right parotid tumor in a 67-year-old woman was initially diagnosed as a salivary gland neoplasm of uncertain malignant potential, favoring an adenoid cystic carcinoma. Subsequent parotidectomy identified an encapsulated basal cell adenoma [Figure 8]. The tumor exhibited monomorphic basaloid cells with ductal differentiation and a strong membranous beta-catenin expression pattern. Molecular testing revealed a *CTNNB1* p.I35T mutation. Ancillary molecular testing may have been useful in determining a more accurate risk of malignancy to guide patient surgical management.

Beta-catenin expression and mutations in *CTNNB1*, its
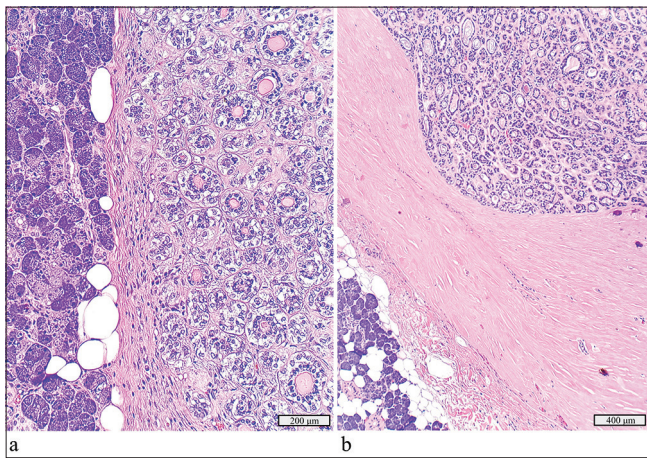
Figure 7: Adenoid cystic carcinoma ex pleomorphic adenoma with a detected *HRAS* p.Q61L mutation. (a) Focus of the adenoma component juxtaposed with benign salivary gland, hematoxylin and eosin stain, ×20 objective. (b) Focus of the adenoid cystic carcinoma component, hematoxylin and eosin stain, ×10 objective.

Figure 8: Basal cell adenoma with a detected *CTNNB1* p.I35T mutation, hematoxylin and eosin stain, ×10 objective.

encoding gene, are specific for basal cell adenoma (present in up to 80%) and have been reported to occur more frequently in adenomas than in basal cell carcinomas.[17] Basal cell carcinomas tend to have more complex molecular profiles, including the accumulation of alterations in *PIK3CA*, *NFKBIA*, and *CYLD*. Therefore, mutations in *CTNNB1* may help differentiate basal cell adenoma from high-grade lesions such as adenoid cystic carcinoma.[10,17]

DISCUSSION

We conducted a feasibility study on a cohort of patients with salivary gland neoplasms to investigate the presence of known cancer-associated gene translocations, deletions, insertions, single nucleotide variants, and copy number changes and to assess the utility of RNA sequencing results to guide management and targeted therapy. The molecular alterations identified in these cases had the potential to have significantly influenced patient management.[18-20] Implementing a comprehensive RNA-based sequencing panel in-house, alongside existing clinical assays, proved feasible. In the era of precision medicine, selecting patients based on molecular profiling enhances the risk of malignancy stratification and supports novel therapeutic strategies.[18-20] Although we used residual resection specimens, we advocate for such testing in FNAC and small biopsies, where accurate initial diagnoses are crucial for guiding patient follow-up, surgical management, and emerging targeted therapies.

RNA-based NGS is a robust technique for analyzing structural gene rearrangements, mutations, and gene copy number changes.[21] It offers significant advantages over single-gene testing methods such as immunohistochemistry, FISH, or real-time PCR, particularly when working with limited material from FNAC and small biopsies. Large RNA-based panels can provide a comprehensive evaluation of the transcriptome, enabling simultaneous examination of multiple genes.[21] This high-throughput approach not only maximizes the utility of limited tissue samples by reducing the need for multiple individual tests but also lowers the overall cost of comprehensive genetic testing for patients.[22,23]

Archer FusionPlex assays employ anchored multiplex PCR technology to enrich specific genomic regions using gene region-specific primers designed to bind known 3' and 5' sites.[24] This targeted enrichment enhances the sensitivity of downstream analyses, even when starting with small quantities of material, such as from FNAC small biopsies and fragmented nucleic acids preserved in FFPE samples. By utilizing a diverse array of primers with anchored sequences, the assays can cover a wide range of potential fusion partners.[24] This approach enables the detection of both known and novel structural gene rearrangements, even without prior knowledge of the fusion partners. This provides a distinct advantage over techniques that depend on known breakpoints.[24]

The main limitation to the Archer FusionPlex Pan Solid Tumor v2 panel is that it does not detect gene fusions located outside of the targeted gene regions. In addition, when the positive selection criteria defined for a "strong-evidence fusion" is not met, but qualifiable data for a "weak-evidence fusion" are found, it can be difficult to determine whether the findings are reportable without repeat testing or confirmation by an orthogonal method.[25]

Implementing molecular assays for rare neoplasms is challenging due to their low case volumes. In our multi-hospital system, the extensive caseload across our pathology departments makes assay validation feasible, but integrating these assays into routine workflows is not cost-effective and poses compliance challenges without batching samples. Our study demonstrates that batch processing with assays using the same proprietary chemistry, such as the Archer FusionPlex Pan Solid Tumor v2 panel RNA-based sequencing, can be effective. This panel aligns with our current Archer FusionPlex CTL kit, simplifying future integration and staff training. As a proof of concept, we tested lung adenocarcinoma cases with known *MET* exon 14 mutations alongside salivary gland specimens using molecular barcodes. This approach enables us to batch rare salivary gland cases with weekly or biweekly runs of lung and thyroid cancer specimens, optimizing time and resources. With this batched testing model, we expect a turnaround time of 10 working days or less, showcasing the efficiency of an in-house panel compared to external services. This method offers better control over pre-analytic variables, ensures proper tissue stewardship, and reduces transportation costs and delays, while the RNA-based NGS assay covers relevant gene targets across various cancer types, facilitating a unified workflow for fusion detection.

Our study focused on FFPE surgical specimens primarily due to their widespread availability. According to the manufacturer, Archer FusionPlex assays can be applied to a range of sample types, including cell cultures, fresh tissues, frozen tissues, and isolated RNA samples. However, it is important to highlight the potential benefits of using an RNA-based molecular sequencing panel for other specimen types commonly encountered in diagnostic laboratories, such as FNAC and small biopsy specimens. These specimens can be submitted in various forms, including aspirate-smeared slides, cytospin slides, or residual samples in CytoLyt solution. Recent research has demonstrated that RNA extraction and sequencing from different cytology preparations can be highly effective.[26-28] Furthermore, although other sample preparation types such as fresh and snap-frozen biopsy samples may present logistical challenges, incorporating these into testing protocols could also enhance the ability to sequence high-quality nucleic acids.[29]

At our institution, we propose using the RNA-based NGS panel for FNAC and small biopsy samples in 2 key scenarios. The first scenario targets cases classified as indeterminate or "salivary gland neoplasms of uncertain malignant potential" under the Milan System for Reporting Salivary Gland Cytopathology, where identifying specific molecular markers could aid in diagnosing and classifying the neoplasm. The second scenario involves known malignant samples, where molecular testing could offer crucial prognostic and predictive biomarker information to enhance patient management.[18-20] Conducting molecular testing on the initial diagnostic sample can provide crucial information for guiding neoadjuvant therapy options, informing surgical decision-making, and offering targeted treatment strategies for tumors that are not resectable.[18-20]

Our study was constrained by a relatively small cohort size (*n* = 17) due to the limited availability of residual material from salivary gland cases for testing. While this small sample size provides preliminary insights, it also presents several limitations. The findings may not be broadly generalizable to the wider population of salivary gland neoplasms and may not capture rare variants effectively. For robust validation and to ensure that our results are applicable to a broader range of salivary gland tumors, further experiments will need to include a larger sample size.

Future studies will aim to include a broader range of tumor types for fusion testing. To strengthen validation efforts, we plan to correlate RNA-based NGS results with other testing methods such as FISH, PCR, and immunohistochemistry (e.g., PLAG1 and MYB). Expanding our validation to different sample preparations, including cytology aspirate smears and liquid preparations, could enhance the clinical applicability of our findings. In addition, with the growing interest in liquid biopsies, it would be valuable to investigate peripheral blood for circulating tumor DNA (ctDNA) and RNA (ctRNA) in our patient cohort.[30] Advances in NGS technology now enable the detection of very low levels of ctDNA and ctRNA from peripheral blood samples, which can aid in monitoring treatment response, detecting minimal residual disease and early recurrence, and providing prognostic information.[31]

SUMMARY

In this proof-of-concept study, a large RNA-based NGS cancer panel effectively detected diagnostic and actionable gene translocations and mutations in salivary gland neoplasms using stored FFPE tissue. About half of the successfully sequenced cases from our cohort showed cancer-associated gene alterations with diagnostic, prognostic, or therapeutic potential. We propose that ancillary molecular testing can enhance the accuracy of salivary gland FNAC and small biopsies, leading to better-informed patient management and personalized care. This study also demonstrated the feasibility of integrating targeted RNA sequencing for fusion testing into routine clinical laboratory workflows.

AVAILABILITY OF DATA AND MATERIALS

All data generated or analyzed during this study are included in this article. Further inquiries can be directed to the corresponding author.

ABBREVIATIONS

NGS – Next-generation sequencing;
FNAC – Fine needle aspiration cytology;
FFPE – Formalin-fixed paraffin-embedded;
BCL – Binary base call;
CTL – FusionPlex Comprehensive Thyroid and Lung;
FISH – Fluorescent in situ hybridization;
RT-PCR – Real-time polymerase chain reactiom;
ctDNA – Circulating tumor DNA;
ctRNA – Circulating tumor RNA

AUTHOR CONTRIBUTIONS

GHS: Conceptualization, data curation, formal analysis, investigation, methodology, project administration, visualization, writing original draft preparation, writing — review and editing; JH: Data curation, visualization, formal analysis, writing – original draft preparation, writing – review and editing; DM: Conceptualization, visualization, data curation, writing – review and editing; JS.T: Supervision; conceptualization; formal analysis; methodology; project administration; writing – original draft preparation writing –reviewing and editing.

ETHICS APPROVAL AND CONSENT TO PARTICIPATE

Human subjects research was involved in this study and was carried out in compliance with the Helsinki Declaration with review and oversight from the institutional review board of the Houston Methodist Research Institute. The study was approved for a waiver of informed consent in November 2022 by the Institutional Review Board at Houston Methodist Research Institute (ethical approval no: protocol 00035700).

ACKNOWLEDGMENT

FUNDING

CONFLICT OF INTEREST

The authors declare no conflict of interest.

EDITORIAL/PEER REVIEW

To ensure the integrity and highest quality of CytoJournal publications, the review process of this manuscript was conducted under a **double-blind model** (authors are blinded for reviewers and vice versa) through an automatic online system.

REFERENCES

1. Pusztaszeri M, Rossi ED, Faquin WC. Update on salivary gland fine-needle aspiration and the Milan System for Reporting Salivary Gland Cytopathology. Arch Pathol Lab Med 2024;148:1092-104.
2. Skalova A, Hyrcza MD. Proceedings of the North American Society of Head and Neck Pathology Companion Meeting, New Orleans, LA, March 12, 2023: Classification of salivary gland tumors: Remaining controversial issues? Head Neck Pathol 2023;17:285-91.
3. Moutasim KA, Thomas GJ. Salivary gland tumours: Update on molecular diagnostics. Diagn Histopathol 2020;26:159-64.
4. World Medical Association. World Medical Association Declaration of Helsinki. Ethical principles for medical research involving human subjects. Bull World Health Organ 2001;79:373-4.
5. Christensen PA, Subedi S, Pepper K, Hendrickson HL, Li Z, Thomas JS, *et al.* Development and validation of Houston Methodist Variant Viewer version 3: Updates to our application for interpretation of next-generation sequencing data. JAMIA Open 2020;3:299-305.
6. Harrison PW, Amode MR, Austine-Orimoloye O, Azov AG, Barba M, Barnes I, *et al.* Ensembl 2024. Nucleic Acids Res 2024;52:D891-9.
7. Altschul SF, Gish W, Miller W, Myers EW, Lipman DJ. Basic local alignment search tool. J Mol Biol 1990;215:403-10.
8. Humtsoe JO, Kim HS, Jones L, Cevallos J, Boileau P, Kuo F, *et al.* Development and characterization of MYB-NFIB fusion expression in adenoid cystic carcinoma. Cancers (Basel) 2022;14:2263.
9. Adderley H, Rack S, Hapuarachi B, Feeney L, Morgan D, Hussell T, *et al.* The utility of TP53 and PIK3CA mutations as prognostic biomarkers in salivary adenoid cystic carcinoma. Oral Oncol 2021;113:105095.
10. Toper MH, Sarioglu S. Molecular pathology of salivary gland neoplasms: Diagnostic, prognostic, and predictive perspective. Adv Anat Pathol 2021;28:81-93.
11. Nakaguro M, Tada Y, Faquin WC, Sadow PM, Wirth LJ, Nagao T. Salivary duct carcinoma: Updates in histology, cytology, molecular biology, and treatment. Cancer Cytopathol 2020;128:693-703.
12. Gouda MA, Subbiah V. Precision oncology for BRAF-mutant cancers with BRAF and MEK inhibitors: From melanoma to tissue-agnostic therapy. ESMO Open 2023;8:100788.
13. Ni W, Chen Z, Zhou X, Yang R, Yu M, Lu J, *et al.* Targeting

Notch and EGFR signaling in human mucoepidermoid carcinoma. Signal Transduct Target Ther 2021;6:27.

14. Chen Z, Ni W, Li JL, Lin S, Zhou X, Sun Y, *et al.* The CRTC1-MAML2 fusion is the major oncogenic driver in mucoepidermoid carcinoma. JCI Insight 2021;6:e139497.

15. Hanna GJ, Guenette JP, Chau NG, Sayehli CM, Wilhelm C, Metcalf R, *et al.* Tipifarnib in recurrent, metastatic HRAS-mutant salivary gland cancer. Cancer 2020;126:3972-81.

16. Rieke DT, Schröder S, Schafhausen P, Blanc E, Zuljan E, von der Emde B, *et al.* Targeted treatment in a case series of AR+, HRAS/PIK3CA co-mutated salivary duct carcinoma. Front Oncol 2023;13:1107134.

17. Oh KY, Hong SD. Infarction of basal cell adenoma of the parotid gland: First case report and literature review on CTNNB1 I35T mutations in salivary basal cell neoplasms. Oral Oncol 2023;145:106534.

18. Rack S, Feeney L, Hapuarachi B, Adderley H, Woodhouse L, Betts G, *et al.* Evaluation of the clinical utility of genomic profiling to inform selection of clinical trial therapy in salivary gland cancer. Cancers (Basel) 2022;14:1133.

19. Pang J, Houlton JJ. Management of malignant salivary gland conditions. Surg Clin North Am 2022;102:325-33.

20. Rached L, Saleh K, Casiraghi O, Even C. Salivary gland carcinoma: Towards a more personalised approach. Cancer Treat Rev 2024;124:102697.

21. Gondane A, Itkonen HM. Revealing the history and mystery of RNA-seq. Curr Issues Mol Biol 2023;45:1860-74.

22. Arriola E, Bernabé R, Campelo RG, Biscuola M, Enguita AB, López-Ríos F, *et al.* Cost-effectiveness of next-generation sequencing versus single-gene testing for the molecular diagnosis of patients with metastatic non-small-cell lung cancer from the perspective of Spanish reference centers. JCO Precis Oncol 2023;7:e2200546.

23. Sheffield BS, Eaton K, Emond B, Lafeuille MH, Hilts A, Lefebvre P, *et al.* Cost savings of expedited care with upfront next-generation sequencing testing versus single-gene testing among patients with metastatic non-small cell lung cancer based on current Canadian practices. Curr Oncol 2023;30:2348-65.

24. Kumbrink J, Demes MC, Jeroch J, Bräuninger A, Hartung K, Gerstenmaier U, *et al.* Development, testing and validation of a targeted NGS-panel for the detection of actionable mutations in lung cancer (NSCLC) using anchored multiplex PCR technology in a multicentric setting. Pathol Oncol Res 2024;30:1611590.

25. Fujita S, Masago K, Sasaki E, Tsukushi S, Horio Y, Kuroda H, *et al.* Weak-evidence fusion candidates detected by a FusionPlex assay using the ion torrent system. *In Vivo* 2021;35:993-8.

26. Ramani NS, Chen H, Broaddus RR, Lazar AJ, Luthra R, Medeiros LJ, *et al.* Utilization of cytology smears improves success rates of RNA-based next-generation sequencing gene fusion assays for clinically relevant predictive biomarkers. Cancer Cytopathol 2021;129:374-82.

27. Sorber L, Claes B, Zwaenepoel K, Van Dorst B, De Winne K, Fransen E, *et al.* Evaluation of cytologic sample preparations for compatibility with nucleic acid analysis. Am J Clin Pathol 2022;157:293-304.

28. Pisapia P, Pepe F, Sgariglia R, Nacchio M, Russo G, Conticelli F, *et al.* Next generation sequencing in cytology. Cytopathology 2021;32:588-95.

29. Chen YY, Han QY, Chen QY, Zhou WJ, Zhang JG, Zhang X, *et al.* Impact of sample processing and storage conditions on RNA quality of fresh-frozen cancer tissues. Biopreserv Biobank 2023;21:510-7.

30. Baev V, Koppers-Lalic D, Costa-Silva B. Liquid biopsy: Current status and future perspectives. Cancers (Basel) 2023;15:3205.

31. Brockley LJ, Souza VG, Forder A, Pewarchuk ME, Erkan M, Telkar N, *et al.* Sequence-based platforms for discovering biomarkers in liquid biopsy of non-small-cell lung cancer. Cancers (Basel) 2023;15:2275.